Published in final edited form as:
Cancer Res. 2009 July 1; 69(13): 5610–5617. doi:10.1158/0008-5472.CAN-08-4967.

Harnessing competing endocytic pathways for overcoming the tumor-blood barrier: MRI and NIR imaging of bifunctional contrast media

Helena Sheikhet Migalovich[1], **Vyacheslav Kalchenko**[2], **Nava Nevo**[1], **Gila Meir**[1], **Fortune Kohen**[1], and **Michal Neeman**[1]

[1] Department of Biological Regulation, The Weizmann Institute of Science, Rehovot 76100 Israel

[2] Department of Veterinary Resources, The Weizmann Institute of Science, Rehovot 76100 Israel

Abstract

Ovarian cancer is the most lethal gynecological malignancy, often diagnosed at advanced stage leading to poor prognosis. In the study reported here, MRI and NIR imaging were applied for in vivo analysis of two competing endocytic pathways affecting retention of bifunctional daidzein-BSA based contrast media by human epithelial ovarian carcinoma cells. Suppression of caveolae mediated uptake using nystatin or by BSA competition significantly enhanced daidzein-BSA-GdDTPA/CyTE777 uptake by tumor cells in vitro. In vivo, perivascular myofibroblasts generated an effective barrier excluding delivery of BSA-GdDTPA/CyTE777 to tumor cells. The ability to manipulate caveolae-mediated sequestration of albumin by perivascular tumor myofibroblasts allowed to effectively overcome this tumor-stroma barrier, increasing delivery of daidzein-BSA-GdDTPA/CyTE777 to the tumor cells in tumor xenografts. Thus, both in vitro and in vivo, endocytosis of daidzein-BSA-GdDTPA/CyTE777 by ovarian carcinoma cells was augmented by albumin or by nystatin. In view of the cardinal role of albumin in affecting the availability and pharmacokinetics of drugs, this approach could potentially also facilitate the delivery of therapeutics and contrast media to tumor cells.

Keywords

Molecular imaging; MRI; ovarian cancer

Introduction

Ovarian cancer is the most lethal gynecological malignancy, placing it among the five most common causes of cancer-induced deaths in women. Ovarian cancer is often detected at advanced stage, and despite frequent effective response to initial chemotherapy, clinical prognosis is poor (1). We have previously reported the contribution of LH and FSH in induction of angiogenesis and adhesion of ovarian carcinoma tumors (2). Furthermore, using MRI, we showed that angiogenesis and progression in ovarian carcinoma is tightly linked spatially and temporally with desmoplastic reaction associated with fibroblasts and myofibroblasts recruited to the tumors (3)(4) (5).

Corresponding author: Prof. Michal Neeman, Department of Biological Regulation, Weizmann Institute, Rehovot 76100 Israel, Tel/Fax 972-8-9342487, Email michal.neeman@weizmann.ac.il.

BSA-GdDTPA/FAM was previously applied for MRI and fluorescence imaging of vascular permeability associated with angiogenesis in tumors (6), grafts(7), and pregnancy(8). Additionally, we recently reported the use of biotin-BSA-GdDTPA for tracking tumor stroma fibroblasts by MRI (9,10). Due to the central role of albumin in affecting the pharmacokinetics of chemotherapeutics and contrast media, we evaluated the fate of biotin-BSA-GdDTPA extravasated from leaky blood vessels in ovarian carcinoma tumor xenografts. Histological staining of the biotinylated albumin based contrast material showed lymphatic clearance, along with residual prolonged retention within the myofibroblast stroma tracks, where it was internalized by alpha smooth muscle actin expressing myofibroblasts. Subsequent in vitro studies showed that biotin-BSA-GdDTPA was effectively internalized by fibroblasts using caveolae mediated uptake, which could be suppressed by treatment with nystatin(9), (11). Upon internalization, the material is sequestered within small intracellular vacuoles leading to suppressed MRI relaxivity, which is regained only after the material is redistributed in the cells with cell division (12) (9). The contrast material did not extravasate into the interstitial space within the tumor nodules (9). The exclusion of the contrast media from the tumor nodules suggested that interaction of therapeutics or contrast media with albumin could significantly hinder their delivery to the tumor cells.

In the study reported here, we aimed to alter the distribution of biotin-BSA-GdDTPA, and to enhance the partition of the contrast material to the tumor by addition of daidzein as a targeting ligand, recently reported to show high affinity to the ovarian carcinoma cells (13). A carboxyalkyl derivative of the isoflavone daidzein, was used since isoflavones interact weakly with ER and have additional cellular activities not ascribed to activation of the ERs, such as regulation of cell-signaling pathways, and can inhibit proliferation and induce apoptosis in ER-negative breast cancer cell lines (e.g., MDA-MB-231), as well as in ER-positive lines (e.g., MCF-7) (14). It was recently reported that the N-t-Boc-hexylenediamine derivative of 7-(O)-carboxymethyl daidzein exhibits more potent inhibitory activity on the growth of estrogen sensistive (eg ovarian, colon) cancer cell lines than the parent isoflavones while retaining no estrogenic activity. As recently reported, the antiproliferative effects of this compound, was also effective *in vivo* in reducing growth of human ovarian xenografts in nude mice (15). Daidzein-BSA-GdDTPA/CyTE-777 conjugate was generated and applied here for MRI/NIR detection of ovarian carcinoma tumors in vivo, while daidzein-BSA-FAM and BSA-ROX were used for in vitro analysis of endocytosis of the contrast media by fluorescence microscopy and by flow cytometry. This work adds daidzein to a rapidly growing list of ligands that are being developed for targeted imaging of tumors by MRI, including targeting glutamine transporters (16), folate receptors (17), and Her-2/neu receptors (18).

We report here that the use of daidzein-BSA-GdDTPA/CyTE-777 (or FAM) as a bifunctional targeted contrast media revealed a novel mechanism regulating endocytosis by ovarian cancer cells, involving competition between receptor mediated internalization through binding of daidzein and caveolae mediated internalization via binding of albumin. Thus, internalization of daidzein-BSA- GdDTPA/CyTE-777 (or FAM) could be induced by competition with BSA CyTE-777 (or ROX), or alternatively by inhibition of caveolae uptake using nystatin. Histological analysis of tumors revealed significant uptake of the bifunctional contrast media to the tumor cells, overcoming the limited distribution observed for biotin-BSA-GdDTPA, which is restricted to the perivascular stroma cells. These results provide a mechanism for altering the micro-distribution and partition of the contrast media within the tumor, achieving effective targeting of the tumor cells, and providing possibilities for modulating the delivery through exogenous competition with caveolae mediated binding of albumin.

Materials and methods

Reagents

BSA, nystatin, polylysine, DTPA anhydride, $GdCl_3$, and DAPI were purchased from Sigma-Aldrich (St. Louis, MO). FAM-NHS and ROX-NHS were purchased from Molecular Probes, Invitrogen, (California, USA). N-1-(p-isothiocyanatophenyl) diethylenetriamine- N^1,N^2,N^3-tetraacetate (DTTA), chelated with Eu^{3+} (EuDTTA) and enhancement solution were obtained from Perkin-Elmer (Turku, Finland). Goat-anti-rabbit peroxidase and goat anti-mouse peroxidase were obtained from (Zymed, USA). Rabbit anti-caveolin1 antibody was purchased from Santa-Cruz (California, USA).

Contrast media

Daidzein-BSA-GdDTPA—BSA-DTPA was synthesized as described (19). Briefly, DTPA anhydride 1.6 gr (suspended in 4 ml of dry DMF) was slowly added with stirring to BSA 1.3gr (in 40 ml Hepes 0.1M, pH 8.8) while the reaction was titrated with NaOH 5N and stirred for 2 hours. The product was dialyzed against $NaHCO_3$. Afterwards, the N-hydroxysuccinimide ester of 7-(O)-carboxymethyl (daidzein-NHS), synthesized according to reference (15), (11 mg in 800 μl of anhydrous DMF) was added to BSA-DTPA (in 40 ml of $NaHCO_3$, 0.1M, pH 8.5) and stirred overnight. The product was dialyzed (19) first against $NaHCO_3$, followed by sodium citrate (0.1 M, pH 6.5). $GdCl_3$ 650 mg (in 5 ml sodium acetate 0.1M, pH6.0) was added to Daidzein-BSA-DTPA in sodium citrate (0.1 M pH6.5). The final product (Daidzein-BSA-GdDTPA) was dialyzed extensively against water and lyophilized.

BSA- CyTE-777/FAM/ROX—CyTE-777-NHS (44 mg) prepared according to (20) or FAM-NHS (35 mg) or ROX-NHS (35 mg) (in 200 μl dry DMF) were added to BSA (450 mg) (in 15 ml $NaHCO_3$, 0.1M, pH 8.5), slowly with stirring. The reaction was stirred overnight, and the product was dialyzed against $NaHCO_3$, 0.1M, pH 8.5, followed by several changes of water and lyophilized.

Daidzein-BSA-CyTE-777/FAM—daidzein-NHS (8 mg) (in 600 μl dry DMF), was added to BSA-CyTE-777/FAM (100 mg; in 6 ml of $NaHCO_3$, 0.1M, pH 8.5), and the reaction was stirred overnight. The product was purified by dialysis against $NaHCO_3$, 0.1M, pH 8.5, followed by several changes of water and lyophilized. This product was used for the in vivo studies.

Fluorescence microscopy

MLS cells ($2*10^5$) were cultured on polylysine coated coverslips for 48h. Subsequently, the coverslips were incubated for 1 hour at 37° with Daidzein-BSA-FAM (200 μg/ml) or BSA-FAM (200 μg/ml) or combination of both (Daidzein-BSA-FAM with BSA-ROX) in the presence or absence of a blocking dose of nystatin (50 μg/ml). The excess of fluorescent material was washed 3 times with PBS, and the cells were fixed with 4% PFA, then washed, and stained with DAPI and mounted. The images were monitored by two-photon microscopy (2PM; Zeiss LSM 510 META NLO; equipped with a broadband Mai Tai-HP-femtosecond single box tunable Ti-sapphire oscillator, with automated broadband wavelength tuning 700–1,020 nm from Spectraphysics, for two-photon excitation).

Histological sections of isolated tumors, from mice injected with Daidzein-BSA-FAM or BSA-FAM or combination of Daidzein-BSA-FAM and BSA-ROX, were deparafinized, stained with DAPI and mounted. The fluorescence signal was monitored by confocal microscopy (Zeiss LSM 710).

Flow cytometry

MLS cells (10^6) were incubated for 30 minutes with Daidzein-BSA-FAM (200 μg/ml) or BSA-ROX (200 μg/ml) or a combination of both in the presence or absence of a blocking dose of nystatin (50 μg/ml). The excess of fluorescent material was washed three times with PBS containing 0.01% of sodium azide. The cellular uptake of fluorescent material was monitored by FACScan (Becton Dickinson, USA). The excitation produced by air-cooled argon laser 288 nm and the emission signal was collected by FL1 filter (BP530/30) for FAM and FL2 filter (BP585/42) for ROX.

Animal experiments

All animal experiments were approved by the Animal Care and Use Committee of Weizmann Institute. CD-1 nude mice were inoculated s.c. with $2.5 \cdot 10^6$ MLS tumor cells. Tumors were allowed to grow until 5–7 mm in diameter (approximately 14–21 days).

In vivo NIR imaging

Tumor bearing mice were injected with daidzein-BSA-CyTE-777 (i.v.; 1mg (for IVIS 100) or 0.5mg (for IVIS Spectrum) in 0.1 ml PBS/mouse; n=5 and n=2 respectably); or with BSA-CyTE-777 (1mg or 0.5mg in 0.1ml PBS/mouse; n=2 and n=2) as control, or with daidzein-BSA-CyTE-777 + BSA-FAM (1mg (for IVIS 100) or 0.5mg (for IVIS Spectrum) of each dye in 0.1ml PBS/mouse; n=2 and n=2 respectably; for the BSA overload experiment). The NIR signal in the whole animal was monitored by IVIS 100 and IVIS Spectrum (Xenogen, Caliper) at 24, 48 and 72h. The mice were fed with alfalfa-free (chlorophyll- free) diet 72h pre visualization. In the IVIS 100 the data was acquired by 710–760 excitation, 675–720 excitation background and 810–860 emission filters. In the IVIS Spectrum the data obtained for the daidzein-BSA-CyTE-777 was acquired by 745 nm excitation and 820 nm emission filters.

The pharmacokinetics of the fluorescent and MRI BSA based contrast media and their plasma concentration after intravenous administration were previously reported to be similar for all tags (19).

MRI measurements

MRI experiments were performed on a horizontal 4.7 T Biospec spectrometer (Bruker, Karlsruhe) using an actively radio-frequency decoupled 1.5 cm surface coil embedded in a Perspex board and a birdcage transmission coil. *In-vitro:* R_1 measurements spin echo images were acquired at 8 different repetition times ranging between 2000 and 100 ms; 2 averages, field of view 4×4 cm, slice thickness 1 mm, matrix 128 × 128). R_1 relaxation rates for the in vitro experiments were derived by non linear single exponential fitting of images acquired at different repetition times (equation [1]):

$$I = M_0(1 - e^{-TR * R_1}) \quad [1]$$

Where I is the measured signal intensity for each TR and R_1 was derived from optimization of the curve fitting; M_0 is the steady state signal intensity in fully relaxed images.

In-vivo—The tumor bearing mice were injected iv with BSA-GdDTPA (12 mg in 200 μL PBS/mouse) or daidzein-BSA-GdDTPA (12 mg in 200 μL PBS/mouse) or with combination of daidzein-BSA-GdDTPA and BSA-FAM (competition experiment). R_1 was measured 24h, 48h and 72h after injection of the contrast material. T_1 weighted 3D gradient-echo (GE) images, with pulse flip angles of 5°,15°,30°, 50° and 70° were acquired to determined the R_1 values. The acquisition parameters: TR 10ms; TE 3.561ms; 2 averages; field of view 4×4×4;

128×128×128 pixels. Three-dimensional gradient-echo data sets were used for generation of R_1 maps as well as for calculation of the average R_1 values in selected regions of interest by nonlinear best fit to equation [1]:

$$I=M_0 \sin\alpha\,(1-e^{-TR^*R_1})/(1-\cos\alpha\, e^{-TR^*R_1}) \quad [2]$$

Where *I* is the signal intensity as a function of the pulse flip angle. Student's *t* test (two-tailed, equal variance) was used for statistical analysis of the significance of change in relaxation rate between control and labeled tumors.

Results

Presence of caveolin 1 in MLS ovarian cancer cells

When MLS ovarian cells were subjected to SDS-PAGE and probed with an anti caevolin-1, a protein band of 21 kd was visualized by ECL. MCF7-CV1 cells used a positive control showed a protein band with the same MW (Supplementary Figure S1)

Albumin and daidzein mediated labeling of ovarian carcinoma cells: fluorescence microscopy

Endocytic pathways in ovarian cancer cells were evaluated *in-vitro* using two fluorescent probes, mono functional BSA-FAM, targeting cellular caveolae (9), and bifunctional daidzein-BSA-FAM targeting both caveolae and cell surface receptors with affinity to daidzein. Binding and uptake of BSA-FAM and daidzein-BSA-FAM by MLS human epithelial ovarian carcinoma cells could be detected by fluorescence microscopy, showing internalization of the fluorescent probes into intracellular vesicles (Figure 1A). Suppression of caveolae mediated uptake by treatment of the cells with nystatin (50 μg/ml, 30 min), resulted, as expected, in an elevated membrane staining and reduced uptake of BSA-FAM (Figure 1, 2). Surprisingly, nystatin treatment resulted in significantly enhanced internalization of daidzein-BSA-FAM by MLS cells (Figure 1). Thus, albumin binding mediated by caveolae appeared to interfere with internalization of daidzein-BSA-FAM into the cells, despite the role of caveolae uptake of BSA-FAM. To test this hypothesis, we evaluated the ability of BSA to compete with daidzein-BSA-FAM on the albumin binding site in caveolae, thereby facilitating internalization of the material to cells (Figure 2). Here again, internalization of daidzein-BSA-FAM was augmented by addition of nystatin.

Albumin and daidzein mediated endocytosis and labeling of ovarian carcinoma cells: flow cytometry

The binding and uptake of BSA-ROX and daidzein-BSA-FAM by MLS ovarian carcinoma cells was quantified by flow cytometry (figure 3). MLS cells were incubated with either BSA-ROX, daidzein-BSA-FAM, or with both BSA-ROX and daidzein-BSA-FAM in the presence or absence of nystatin. Treatment with nystatin resulted in a significant 4 fold enhancement in the fluorescence intensity of cells incubated with daidzein-BSA-FAM (figure 3A, B). On the other hand, binding and uptake of BSA-ROX were only slightly reduced by nystatin. These results are consistent with a shift from endocytosis to membrane binding of daidzein-BSA-FAM in the presence of nystatin as detected by fluorescence microscopy (Figure 1). Incubation of the cells with both BSA-ROX and daidzein-BSA-FAM resulted in a differential response to nystatin, with increased labeling of cells with daidzein-BSA-FAM (3 fold induction in the intensity and increase of 20% in the population of labeled cells), and decreased fluorescence of BSA-ROX (1.3 fold in intensity and 51% decrease in labeled population) (figure 3B–D). These results are also consistent with the endocytic pathways detected by fluorescence microscopy (Figure 1).

In vivo fluorescence imaging of targeted delivery of daidzein-BSA-CyTE-777 to ovarian carcinoma

Systemic delivery of daidzein-BSA-CyTE-777 resulted is tumor selective enhancement of NIR fluorescence for subcutaneous ovarian carcinoma tumor xenografts (figure 4). Mice were inoculated subcutaneously with $2.5 \cdot 10^6$ MLS tumor cells. Ten days after tumor inoculation, mice administered with daidzein-BSA-CyTE777 or BSA-CyTE777. Already in the first 30 minutes after administration, mice injected with daidzein-BSA-CyTE777 showed more specific localization in the tumor and in higher concentration than mice administered with BSA-CyTE777 (Supplementary Figure S3). Competition of daidzein-BSA-CyTE777 with BSA-ROX overload increased the NIR signal of daidzein-BSA-CyTE777 in the tumor. However, the contrast material distribution was less specific to the tumor itself relative to the injection of daidzein-BSA-CyTE777 alone, suggesting that the endogenous level of albumin may be better optimized for targeted imaging, and BSA overload could reduce specificity by interference with clearance pathways.

Consistent with our hypothesis we observed different pharmacokinetic behavior in the elimination of the contrast materials from the tumor. Control mice injected with BSA-CyTE777 showed first order clearance of the contrast media. Daidzein-BSA-CyTE777 was eliminated with rapid initial kinetics, faster than the elimination rate of BSA-CyTE777. However, this was followed by residual retention of Daidzein-BSA-CyTE777 with very slow clearance. Thus after the initial elimination mice that administered with daidzein-BSA-CyTE777 showed a specific NIR signal in the tumor area that retains for 48 hours after the administration (n=7) and it was statistically significant comparing to the signal of the BSA-CyTE777 injected mice (n=4) (p=0.047) (Figure 4B). The NIR signal in the tumors was detectable even 10 days after the administration.

Biodistribution of daidzein-BSA-EuDTTA (chelate)

The lanthanide chelate of europium (Eu^{3+}) (analog to GdDTPA) has unique fluorescence properties allowing its use for labeling antibodies in immunoassays. MLS tumor bearing mice were injected with BSA-Eu chelate (n=3) or Daidzein-BSA-Eu chelate (n=5). After 24 or 48h the mice were sacrificed and the tumors were isolated. The fluorescence due to Eu in the various extracts of tissues was determined. A large 2 to 3 fold increase in Eu was detected in tumors of the mice injected with Daidzein-BSA-Eu chelate as compared to those injected with BSA-Eu chelate at 24 and 48h after injection. (Figure S2).

Distribution of Daidzein-BSA-FAM in ovarian tumors

The distribution of contrast material inside the tumors was visualized by fluorescence microscopy, in tumors isolated 24 h after injection with daidzein-BSA-FAM or BSA-FAM. Daidzein-BSA-FAM was localized in the tumor cells areas, while BSA-FAM was localized to the tumor blood vessels and their surrounding stroma cells (Figure 5A–B).

Additionally we observe different distribution pattern of daidzein-BSA-FAM or BSA-ROX in the tumor isolated 24h after their combined injection. Consistent with our previous results daidzein-BSA-FAM was distributed in all the tumor area with enhanced staining around the vessel, while BSA-ROX was localized in the stromal fibroblast area. (Figure 5C).

In vivo MRI detection of targeted delivery of daidzein-BSA-CyTE-777 to ovarian carcinoma

Daidzein-BSA-GdDTPA showed significant relaxivity of 194 $mM^{-1}s^{-1}$ (per BSA; Figure 6A). This relaxivity was similar to the relaxivity of BSA-GdDTPA 196 $mM^{-1}s^{-1}$ (per BSA).

MRI data acquired from MLS tumor bearing mice 24h after administration of daidzein-BSA-GdDTPA or BSA-GdDTPA (12 mg/200 μl; n=5–7 per group), showed significantly higher

contrast enhancement, consistent with accumulation of daidzein-BSA-GdDTPA in the tumor site as compared to vehicle-injected mice or mice injected with BSA-GdDTPA (Figure 6B). Time course experiments showed specific localization and retention of targeted contrast agent (daidzein-BSA-GdDTPA; n=7) in the tumor site 24, 48 and 72h after injection as compared to controls or mice injected with non targeted contrast agent (BSA-GdDTPA; n=5). Statistically significant elevation of R_1 relaxation was visualized in tumors injected with daidzein-BSA-GdDTPA as compared to non injected animals or mice injected with BSA-GdDTPA (for 24h p=0.01, 48h p=0.016, 72h p=0.0488; Figure 6C).

Prolonged detection of the targeted contrast material was feasible even for a lower administered dose. MLS tumor bearing mice were injected with daidzein-BSA-GdDTPA (4 mg/200 μl; n=3). The specific localization of the targeted contrast agent in the tumor site was detected by MRI at 9.4T 24h after injection and was still detectable and even enhanced 7 days after injection (Figure 6D; arrows).

The effects of BSA overload were studied on MLS tumor bearing mice injected with daidzein-BSA-GdDTPA (4 mg) or combination of daidzein-BSA-GdDTPA and BSA-FAM. R1 of the tumor area was monitored after 24h. Elevation in R1 was observed for the tumor from animal injected with combination of daidzein-BSA-GdDTPA and BSA-FAM compared to the control animals (supplementary Figure S3).

Discussion

Despite the high permeability tumor neovasculature to plasma proteins, targeting of contrast media and delivery of therapeutics to tumors is frequently compromised leading to poor sensitivity for tumor detection and resistance to therapy. The low transfer rate was attributed to high interstitial pressure, and indeed a number of studies reported improved delivery with vascular normalization induced by antiangiogenic therapy (21), or alteration of extracellular matrix using hyaluronidase (22).

In the study reported here, we explored yet another mechanism for tumor escape from delivery of extravasated albumin based contrast media, through caveolae mediated sequestration of the contrast material by perivascular myofibroblasts, thus generating an effective tumor-blood barrier. Evoking alternate competing endocytic pathway using daidzein resulted in significant partition of the contrast material into the tumor, which could be further enhanced through suppression of caveolae mediated endocytosis by competition with albumin.

The phytoestrogen daidzein bound to bovine serum albumin was used here as a macromolecular bifunctional contrast agent targeting ovarian carcinoma cells. In-vivo imaging of daidzein-BSA- GdDTPA/CyTE-777 allowed MRI and NIR imaging detection and analysis of the interaction between endocytic pathways in MLS human epithelial ovarian carcinoma xenografts.

The *in vitro* use of carboxy derivatives of isoflavones as carriers for affinity targeting of drugs to tumor cells expressing estrogen receptor of the beta type was recently reported (23), (13), (15). Acting as a weak estrogen, daidzein may recognize a putative plasma membrane estrogen receptor and a membrane located ERβ-related protein. Additionally daidzein was reported to interact with the lipid interface on the cell surface (24), thus facilitating endocytosis. It has been reported that caveolin-1 colocalizes with plasma membrane estrogen receptor in lipid rafts (25). Gilad et al. reported the importance of caveolin-1 in the compartmentalization of estrogen receptor beta (ERbeta) to the membrane, allowing 17beta-estradiol (E2) to control vitamin D receptor (VDR) transcription and expression (26). Daidzein could interact also with raft located estrogen receptor like protein which did not cointeract with calveolae (27).

As reported here, MLS human epithelial ovarian carcinoma cells express low levels of caveolin-1 that can mediate the BSA uptake to the MLS cells. As expected, inhibition of caveolae uptake using nystatin, suppressed cellular internalization of fluorescently tagged BSA, and changed the pattern of cellular localization of this agent, leading to membrane staining and inhibition of endocytosis.

Cellular uptake of daidzein-BSA-FAM and BSA-ROX alone and in combination showed segregation of the labels, suggesting independent uptake pathways for daidzein-BSA and BSA. Surprisingly, nystatin significantly augmented the cellular uptake of daidzein-BSA-FAM, whereas the uptake of BSA-ROX was slightly suppressed by nystatin along with a shift towards membranal localization, suggesting that although daidzein-BSA-FAM is internalized through a caveolae independent endocytic pathway, its uptake can be attenuated by the interaction of BSA with caveolin. Similar to the effect of nystatin, administration of BSA-ROX effectively increased daidzein-BSA-FAM uptake. These results are consistent with the presence of two competing and mutually exclusive endocytic pathways for daidzein-BSA-FAM, where one of them is BSA mediated and caveolae dependent, and the second is daidzein mediated and caveolae independent.

In vivo, NIR imaging showed specific localization and prolonged retention of daidzein-BSA-CyTE777 in ovarian carcinoma tumors, compared to BSA-CyTE777. Similarly elevated enhancement of tumors was observed by MRI for daidzein-BSA-GdDTPA relative to BSA-GdDTPA, and contrast media retention in the tumors could be detected up to 7 days after administration of the contrast media. Enhancement of contrast appeared to develop with time after administration. Such behavior is consistent with quenching of relaxivity upon internalization of the contrast media with subsequent enhancement of relaxivity with cell proliferation and intracellular redistribution of the contrast media. Such changes in contrast media relaxivity were previously reported by us for endocytic uptake of BSA-GdDTPA (19) (9,10).

In accord with the *in vitro* results, it is important to consider that retention of the NIR signal in the tumor area is amplified by the intrinsic competition with the endogenous mouse albumin that can compete with daidzein-BSA for uptake by caveolae. Furthermore, uptake of daidzein-BSA could be further amplified by exogenously delivered BSA overload. Further analysis is required in order to establish the optimal concentration of albumin required for maximal delivery of daidzein-BSA. Importantly, hypoalbuminemia (28), a common complication in patients with advanced cancer (29) and a major side effect of some chemotherapeutic agents (30) (31) (32) (33), can affect the delivery of daidzein-BSA, and thus supplementation with exogenous albumin should be considered.

Histological analysis revealed a major difference in the distribution of daidzein-BSA-GdDTPA and BSA-GdDTPA in tumors. Effective distribution of Daidzein-BSA-FAM was observed inside the tumor nodules, while BSA-FAM was predominantly localized within blood vessels and in the perivascular tumor stroma myofibroblasts as reported previously (10).

The study reported here was performed on subcutaneous tumor xenografts that are typically characterized by extensive fibrous reaction. This choice of model facilitated quantification of the contrast media. However, the clinical relevance of the model is nevertheless clear, as extensive involvement of stroma is common to many human carcinomas. Fibroblast involvement was reported for the supportive stroma of breast (34) (35) and prostate (36) (37) carcinomas, contributing to angiogenesis (38), abnormal composition of extracellular matrix (39), and fibrosis development (40).

Targeting caveolae was suggested previously as a mechanism for facilitation of transendothelial transfer so as to improve delivery of therapeutics to tumors (41,42). Similar

to albumin-bound (*nab*™) paclitaxel (*nab*-paclitaxel; Abraxane®) (43) (44) that was recently approved for use in patients with metastatic breast cancer (45), daidzein-BSA shows enhanced endothelial cell transcytosis (44), EPR effect, and prolonged half-life time in the plasma. In addition, daidzein-BSA shows specific affinity to ovarian cancer cells, using intrinsic competition with albumin for saturating the caveolae pathway and enhancing tumor cell uptake. Interestingly, fluorescently labeled Abraxane showed limited partition to the tumor cells and significant perivascular accumulation, suggesting possible uptake by perivascular stroma cells (46).

In summary, we reported here the use of MRI and NIR imaging for *in vivo* dissection of two independent endocytic pathways affecting contrast media retention by human epithelial ovarian carcinoma cells. As shown here, daidzein-BSA-GdDTPA/CyTE-777 could potentially facilitate the detection of ovarian tumor lesions and metastasis, further research is required for validating the ability to detect targeted contrast media for peritoneal metastases. Based in previous reports this system potentially may be used for detection of other types of cancer that are daidzein sensitive, including prostate (47) (48) and breast (49) (50). The mutually exclusive competing mechanisms for daidzein and BSA mediated uptake could be further exploited for augmenting the selective targeted delivery of therapy to ovarian carcinoma cells through suppression of caveolae binding. Moreover, the ability to manipulate caveolae-mediated internalization allowed to effectively overcome the tumor-blood barrier mediated by caveolae sequestration of albumin in perivascular tumor myofibroblasts, thus augmenting delivery of the contrast media to the tumor cells. In view of the cardinal role of albumin in affecting the availability and pharmacokinetics of drugs, this approach could potentially also facilitate the delivery of therapeutics to tumor cells.

Supplementary Material

Refer to Web version on PubMed Central for supplementary material.

Acknowledgments

This work was supported in part by the USA NCI R01 CA75334, by the Yeda CEO fund and by the Gurwin Foundation (to MN), and by equipment support from the Ridgefield Foundation and The ISF Converging Technologies grant. MN is incumbent of the Helen and Morris Mauerberger Chair.

References

1. Lazennec G. Estrogen receptor beta, a possible tumor suppressor involved in ovarian carcinogenesis. Cancer Lett 2006;231:151–7. [PubMed: 16399219]
2. Schiffenbauer YS, Meir G, Maoz M, Even-Ram SC, Bar-Shavit R, Neeman M. Gonadotropin stimulation of MLS human epithelial ovarian carcinoma cells augments cell adhesion mediated by CD44 and by alpha(v)-integrin. Gynecol Oncol 2002;84:296–302. [PubMed: 11812090]
3. Gilead A, Meir G, Neeman M. The role of angiogenesis, vascular maturation, regression and stroma infiltration in dormancy and growth of implanted MLS ovarian carcinoma spheroids. Int J Cancer 2004;108:524–31. [PubMed: 14696116]
4. Neeman M, Dafni H, Bukhari O, Braun RD, Dewhirst MW. In vivo BOLD contrast MRI mapping of subcutaneous vascular function and maturation: validation by intravital microscopy. Magn Reson Med 2001;45:887–98. [PubMed: 11323816]
5. Gilad AA, Israely T, Dafni H, Meir G, Cohen B, Neeman M. Functional and molecular mapping of uncoupling between vascular permeability and loss of vascular maturation in ovarian carcinoma xenografts: the role of stroma cells in tumor angiogenesis. Int J Cancer 2005;117:202–11. [PubMed: 15880497]
6. Dafni H, Landsman L, Schechter B, Kohen F, Neeman M. MRI and fluorescence microscopy of the acute vascular response to VEGF165: vasodilation, hyper-permeability and lymphatic uptake,

followed by rapid inactivation of the growth factor. NMR Biomed 2002;15:120–31. [PubMed: 11870908]

7. Israely T, Nevo N, Harmelin A, Neeman M, Tsafriri A. Reducing ischaemic damage in rodent ovarian xenografts transplanted into granulation tissue. Hum Reprod 2006;21:1368–79. [PubMed: 16459346]
8. Plaks V, Kalchenko V, Dekel N, Neeman M. MRI analysis of angiogenesis during mouse embryo implantation. Magn Reson Med 2006;55:1013–22. [PubMed: 16598729]
9. Granot D, Kunz-Schughart LA, Neeman M. Labeling fibroblasts with biotin-BSA-GdDTPA-FAM for tracking of tumor-associated stroma by fluorescence and MR imaging. Magn Reson Med 2005;54:789–97. [PubMed: 16149062]
10. Granot D, Addadi Y, Kalchenko V, Harmelin A, Kunz-Schughart LA, Neeman M. In vivo imaging of the systemic recruitment of fibroblasts to the angiogenic rim of ovarian carcinoma tumors. Cancer Res 2007;67:9180–9. [PubMed: 17909023]
11. Stuart ES, Webley WC, Norkin LC. Lipid rafts, caveolae, caveolin-1, and entry by Chlamydiae into host cells. Exp Cell Res 2003;287:67–78. [PubMed: 12799183]
12. Geninatti Crich S, Barge A, Battistini E, et al. Magnetic resonance imaging visualization of targeted cells by the internalization of supramolecular adducts formed between avidin and biotinylated Gd3 + chelates. J Biol Inorg Chem 2005;10:78–86. [PubMed: 15616832]
13. Somjen D, Katzburg S, Nevo N, et al. A daidzein-daunomycin conjugate improves the therapeutic response in an animal model of ovarian carcinoma. J Steroid Biochem Mol Biol 2008;110:144–9. [PubMed: 18482833]
14. Harris DM, Besselink E, Henning SM, Go VL, Heber D. Phytoestrogens induce differential estrogen receptor alpha- or Beta-mediated responses in transfected breast cancer cells. Exp Biol Med (Maywood) 2005;230:558–68. [PubMed: 16118406]
15. Kohen F, Gayer B, Kulik T, et al. Synthesis and evaluation of the antiproliferative activities of derivatives of carboxyalkyl isoflavones linked to N-t-Boc-hexylenediamine. J Med Chem 2007;50:6405–10. [PubMed: 17990847]
16. Geninatti Crich S, Cabella C, Barge A, et al. In vitro and in vivo magnetic resonance detection of tumor cells by targeting glutamine transporters with Gd-based probes. J Med Chem 2006;49:4926–36. [PubMed: 16884304]
17. Sun C, Sze R, Zhang M. Folic acid-PEG conjugated superparamagnetic nanoparticles for targeted cellular uptake and detection by MRI. J Biomed Mater Res A 2006;78:550–7. [PubMed: 16736484]
18. Artemov D, Mori N, Ravi R, Bhujwalla ZM. Magnetic resonance molecular imaging of the HER-2/neu receptor. Cancer Res 2003;63:2723–7. [PubMed: 12782573]
19. Dafni H, Gilead A, Nevo N, Eilam R, Harmelin A, Neeman M. Modulation of the pharmacokinetics of macromolecular contrast material by avidin chase: MRI, optical, and inductively coupled plasma mass spectrometry tracking of triply labeled albumin. Magn Reson Med 2003;50:904–14. [PubMed: 14587000]
20. Hilderbrand SA, Kelly KA, Weissleder R, Tung CH. Monofunctional near-infrared fluorochromes for imaging applications. Bioconjug Chem 2005;16:1275–81. [PubMed: 16173808]
21. Bhattacharya A, Seshadri M, Oven SD, Toth K, Vaughan MM, Rustum YM. Tumor vascular maturation and improved drug delivery induced by methylselenocysteine leads to therapeutic synergy with anticancer drugs. Clin Cancer Res 2008;14:3926–32. [PubMed: 18559614]
22. Bouzin C, Feron O. Targeting tumor stroma and exploiting mature tumor vasculature to improve anti-cancer drug delivery. Drug Resist Updat 2007;10:109–20. [PubMed: 17452119]
23. Somjen D, Stern N, Knoll E, et al. Carboxy derivatives of isoflavones as affinity carriers for cytotoxic drug targeting in adrenocortical H295R carcinoma cells. J Endocrinol 2003;179:395–403. [PubMed: 14656209]
24. Lehtonen JY, Adlercreutz H, Kinnunen PK. Binding of daidzein to liposomes. Biochim Biophys Acta 1996;1285:91–100. [PubMed: 8948479]
25. Marquez DC, Chen HW, Curran EM, Welshons WV, Pietras RJ. Estrogen receptors in membrane lipid rafts and signal transduction in breast cancer. Mol Cell Endocrinol 2006;246:91–100. [PubMed: 16388889]

26. Gilad LA, Bresler T, Gnainsky J, Smirnoff P, Schwartz B. Regulation of vitamin D receptor expression via estrogen-induced activation of the ERK 1/2 signaling pathway in colon and breast cancer cells. J Endocrinol 2005;185:577–92. [PubMed: 15930183]
27. Heberden C, Reine F, Grosse B, et al. Detection of a raft-located estrogen receptor-like protein distinct from ER alpha. Int J Biochem Cell Biol 2006;38:376–91. [PubMed: 16263324]
28. Kufe DWP, Raphael E, Weichselbaum Ralph R, Bast Robert C Jr, Gansler Ted S, Holland James F, Frei Emil III. Cancer Medicine. 2003
29. Sharma R, Hook J, Kumar M, Gabra H. Evaluation of an inflammation-based prognostic score in patients with advanced ovarian cancer. Eur J Cancer 2008;44:251–6. [PubMed: 18155897]
30. Atkins MB, Robertson MJ, Gordon M, et al. Phase I evaluation of intravenous recombinant human interleukin 12 in patients with advanced malignancies. Clin Cancer Res 1997;3:409–17. [PubMed: 9815699]
31. Frankel AE, Zuckero SL, Mankin AA, et al. Anti-CD3 recombinant diphtheria immunotoxin therapy of cutaneous T cell lymphoma. Curr Drug Targets 2009;10:104–9. [PubMed: 19199905]
32. Hochhauser D, Meyer T, Spanswick VJ, et al. Phase I study of sequence-selective minor groove DNA binding agent SJG-136 in patients with advanced solid tumors. Clin Cancer Res 2009;15:2140–7. [PubMed: 19276288]
33. Ohnuma T, Holland JF, Freeman A, Sinks LF. Biochemical and pharmacological studies with asparaginase in man. Cancer Res 1970;30:2297–305. [PubMed: 4920133]
34. Bagley RG, Weber W, Rouleau C, Teicher BA. Pericytes and endothelial precursor cells: cellular interactions and contributions to malignancy. Cancer Res 2005;65:9741–50. [PubMed: 16266995]
35. Orimo A, Gupta PB, Sgroi DC, et al. Stromal fibroblasts present in invasive human breast carcinomas promote tumor growth and angiogenesis through elevated SDF-1/CXCL12 secretion. Cell 2005;121:335–48. [PubMed: 15882617]
36. Tuxhorn JA, Ayala GE, Smith MJ, Smith VC, Dang TD, Rowley DR. Reactive stroma in human prostate cancer: induction of myofibroblast phenotype and extracellular matrix remodeling. Clin Cancer Res 2002;8:2912–23. [PubMed: 12231536]
37. McAlhany SJ, Ressler SJ, Larsen M, et al. Promotion of angiogenesis by ps20 in the differential reactive stroma prostate cancer xenograft model. Cancer Res 2003;63:5859–65. [PubMed: 14522910]
38. Kalluri R, Zeisberg M. Fibroblasts in cancer. Nat Rev Cancer 2006;6:392–401. [PubMed: 16572188]
39. Sund M, Kalluri R. Tumor stroma derived biomarkers in cancer. Cancer Metastasis Rev 2009;28:177–83. [PubMed: 19259624]
40. Bergamaschi A, Tagliabue E, Sorlie T, et al. Extracellular matrix signature identifies breast cancer subgroups with different clinical outcome. J Pathol 2008;214:357–67. [PubMed: 18044827]
41. McIntosh DP, Tan XY, Oh P, Schnitzer JE. Targeting endothelium and its dynamic caveolae for tissue-specific transcytosis in vivo: a pathway to overcome cell barriers to drug and gene delivery. Proc Natl Acad Sci U S A 2002;99:1996–2001. [PubMed: 11854497]
42. Carver LA, Schnitzer JE. Caveolae: mining little caves for new cancer targets. Nat Rev Cancer 2003;3:571–81. [PubMed: 12894245]
43. Teneriello MG, Tseng PC, Crozier M, et al. Phase II evaluation of nanoparticle albumin-bound paclitaxel in platinum-sensitive patients with recurrent ovarian, peritoneal, or fallopian tube cancer. J Clin Oncol 2009;27:1426–31. [PubMed: 19224848]
44. Desai N, Trieu V, Yao Z, et al. Increased antitumor activity, intratumor paclitaxel concentrations, and endothelial cell transport of cremophor-free, albumin-bound paclitaxel, ABI-007, compared with cremophor-based paclitaxel. Clin Cancer Res 2006;12:1317–24. [PubMed: 16489089]
45. Perez EA. Impact, mechanisms, and novel chemotherapy strategies for overcoming resistance to anthracyclines and taxanes in metastatic breast cancer. Breast Cancer Res Treat 2009;114:195–201. [PubMed: 18443902]
46. Karmali PP, Kotamraju VR, Kastantin M, et al. Targeting of albumin-embedded paclitaxel nanoparticles to tumors. Nanomedicine 2009;5:73–82. [PubMed: 18829396]
47. Kurahashi N, Iwasaki M, Inoue M, Sasazuki S, Tsugane S. Plasma isoflavones and subsequent risk of prostate cancer in a nested case-control study: the Japan Public Health Center. J Clin Oncol 2008;26:5923–9. [PubMed: 19018085]

48. Singh-Gupta VZH, Banerjee S, Kong D, Raffoul JJ, Sarkar FH, Hillman GG. Radiation-induced HIF-1alpha cell survival pathway is inhibited by soy isoflavones in prostate cancer cells. Int J Cancer 2009;124:1675–84. [PubMed: 19101986]

49. Guha N, Kwan ML, Quesenberry CP Jr, Weltzien EK, Castillo AL, Caan BJ. Soy isoflavones and risk of cancer recurrence in a cohort of breast cancer survivors: the Life After Cancer Epidemiology study. Breast Cancer Res Treat. 2009

50. Eto I. Nutritional and chemopreventive anti-cancer agents up-regulate expression of p27Kip1, a cyclin-dependent kinase inhibitor, in mouse JB6 epidermal and human MCF7, MDA-MB-321 and AU565 breast cancer cells. Cancer Cell Int 2006;6:20. [PubMed: 16899133]

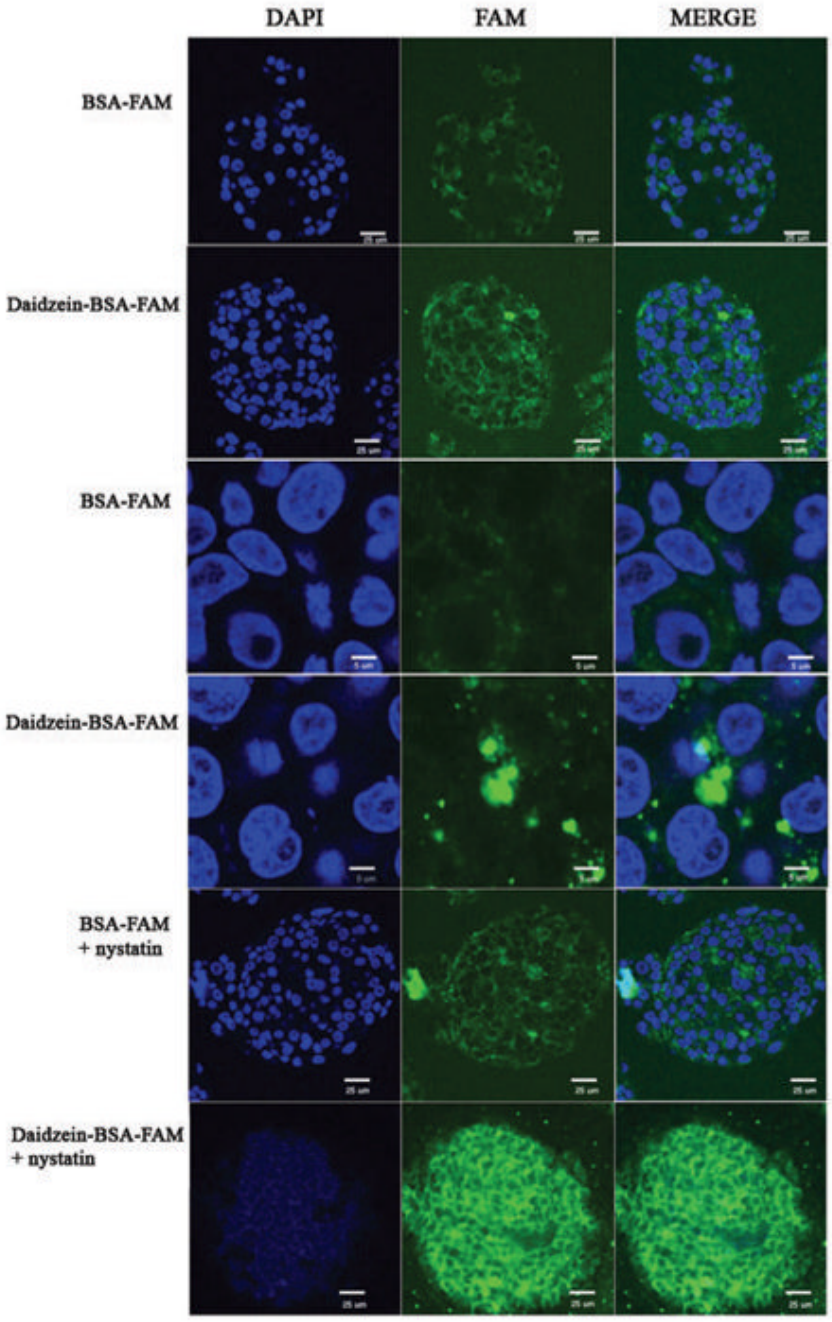

Figure 1. Specific binding and endocytosis of Daidzein-BSA-FAM by MLS ovarian carcinoma cells

Two-photon fluorescence microscopy of MLS human ovarian carcinoma cells incubated (1 h in 37°C) in presence of Daidzein-BSA-FAM (200 μg/ml) or BSA-FAM (200 μg/ml), in the presence or absence of a blocking dose of nystatin (50 μg/ml). Blue, DAPI nuclear staining; green, Daidzein-BSA-FAM or BSA-FAM.

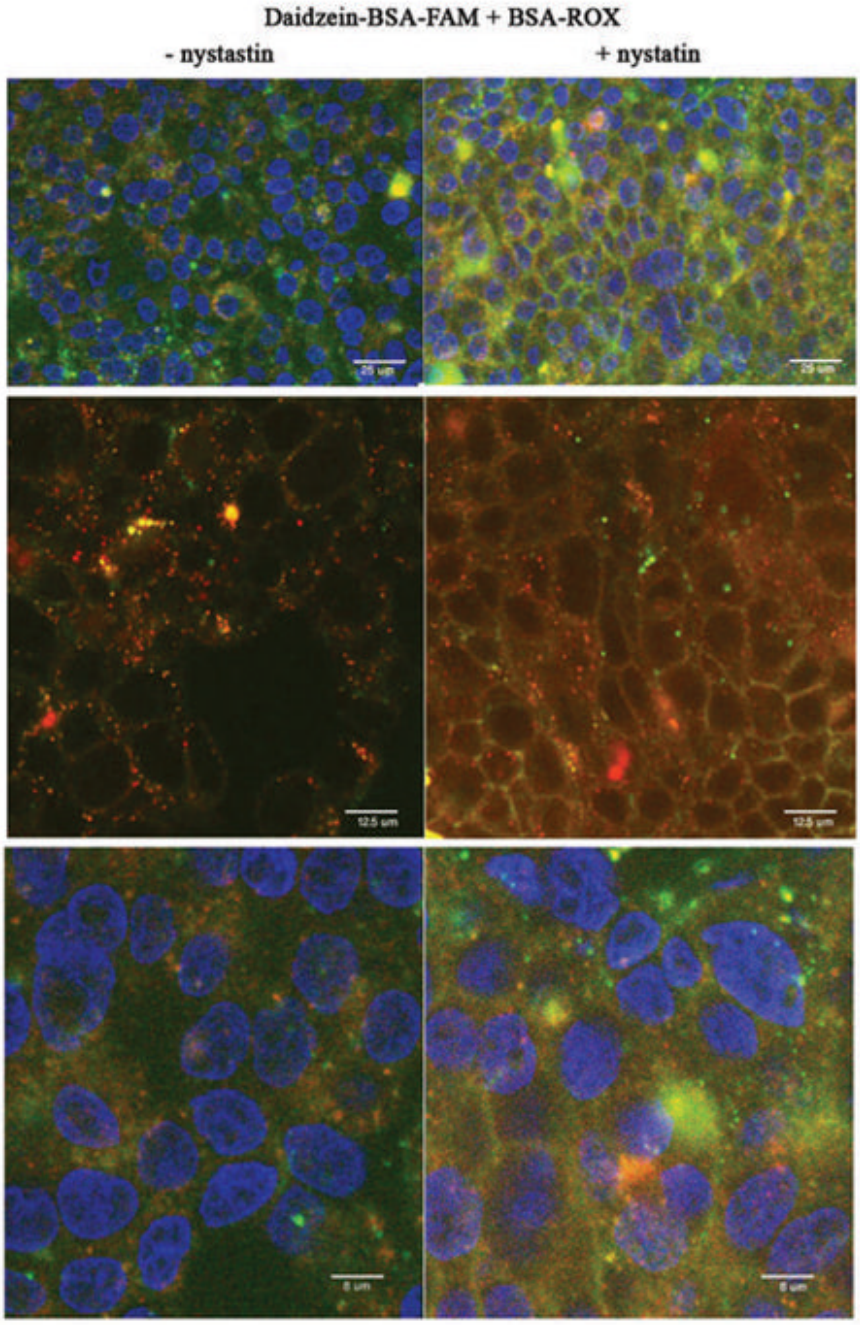

Figure 2. Specific binding and endocytosis of BSA-ROX and Daidzein-BSA-FAM by MLS ovarian carcinoma cells

Two-photon fluorescence microscopy of MLS human ovarian carcinoma incubated for 30 min at 37°C in the presence of (200 μg/ml) Daidzein-BSA-FAM and BSA-ROX (200 μg/ml) with or without inhibition of caveolae mediated uptake using nystatin (50 μg/ml). Green, Daidzein-BSA-FAM; red, BSA-ROX; blue, DAPI nuclear staining.

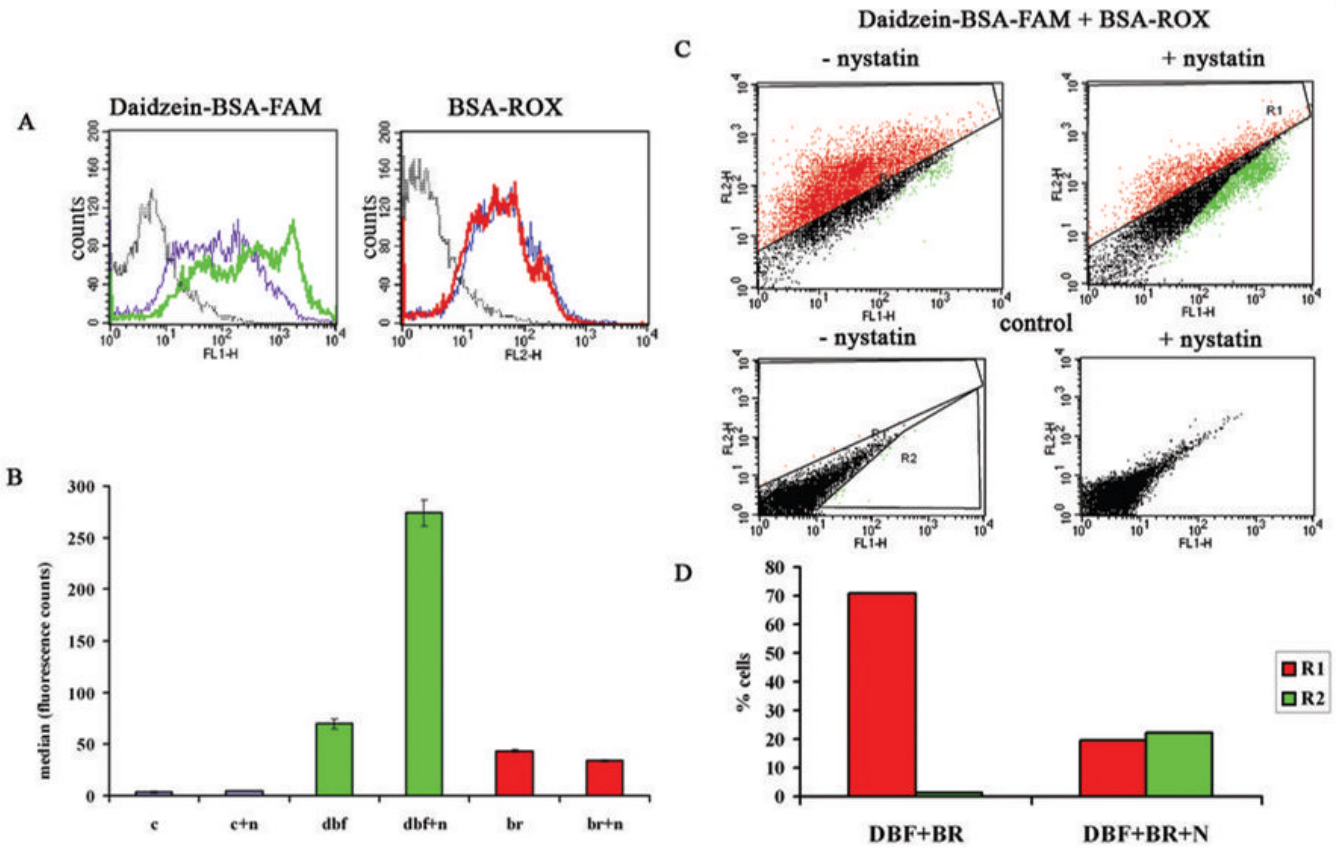

Figure 3. Binding and endocytosis of BSA-ROX and Daidzein-BSA-FAM by MLS ovarian carcinoma cells

Flow cytometry of MLS human ovarian carcinoma incubated for 30 min at 37°C in the presence of (200 μg/ml) Daidzein-BSA-FAM or/and BSA-ROX (200 μg/ml) with or without inhibition of caveolae mediated uptake using nystatin (50 μg/ml) (green-Daidzein-BSA-FAM, red-BSA-ROX). A) Histogram of a) Daidzein-BSA-FAM uptake (grey-control, blue-Daidzein-BSA-FAM uptake, green- Daidzein-BSA-FAM uptake in presence of nystatin), b) BSA-ROX uptake (grey-control, blue- BSA-ROX uptake, red- BSA-FAM uptake in presence of nystatin). B) Statistics median of uptake histogram analysis. C) Competition of Daidzein-BSA-FAM (green) by BSA-ROX (red) in the presence and absence of nystatin (FL1-FAM fluorescence, FL2-ROX fluorescence). D) Statistical analysis of competition assay. Change on percent of positively stained fluorescent cells in absence and presence of nystatin (green-Daidzein-BSA-FAM, red-BSA-ROX).

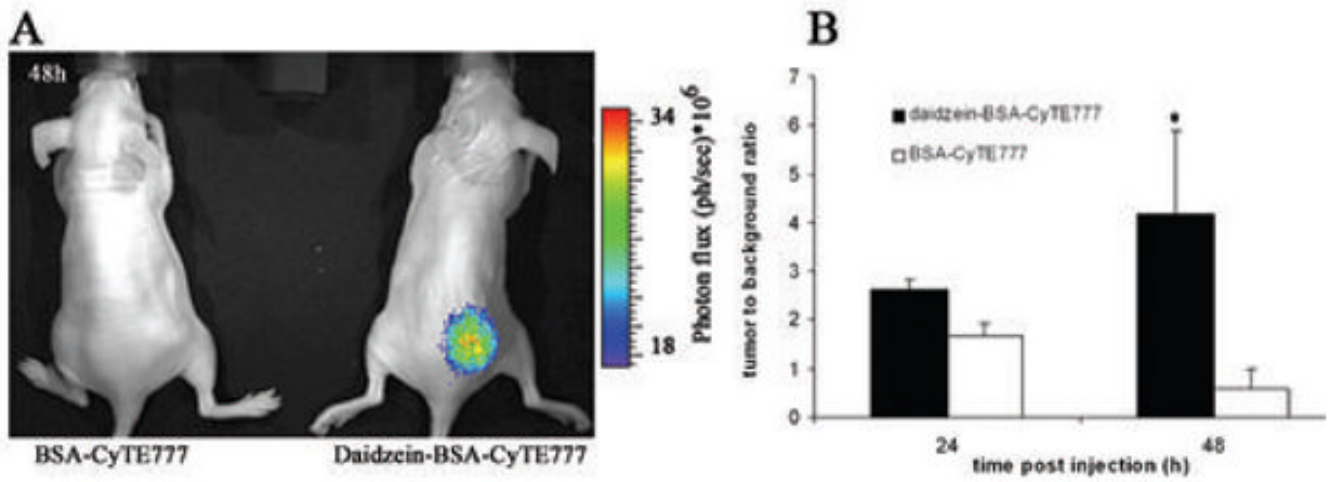

Figure 4. In Vivo NIR Imaging of targeted delivery of daidzein-BSA-CyTE-777 to ovarian carcinoma tumors

A) CD-1 nude mice were inoculated subcutaneously with $2.5*10^6$ cells. When the tumor was visible the mice were administered intravenously with 1) BSA-CyTE-777; 2) daidzein-BSA-CyTE-777. The NIR signal 48 hours after injection is shown. **B)** Elimination of the NIR signal, tumor to background ratio over time. p=0.047

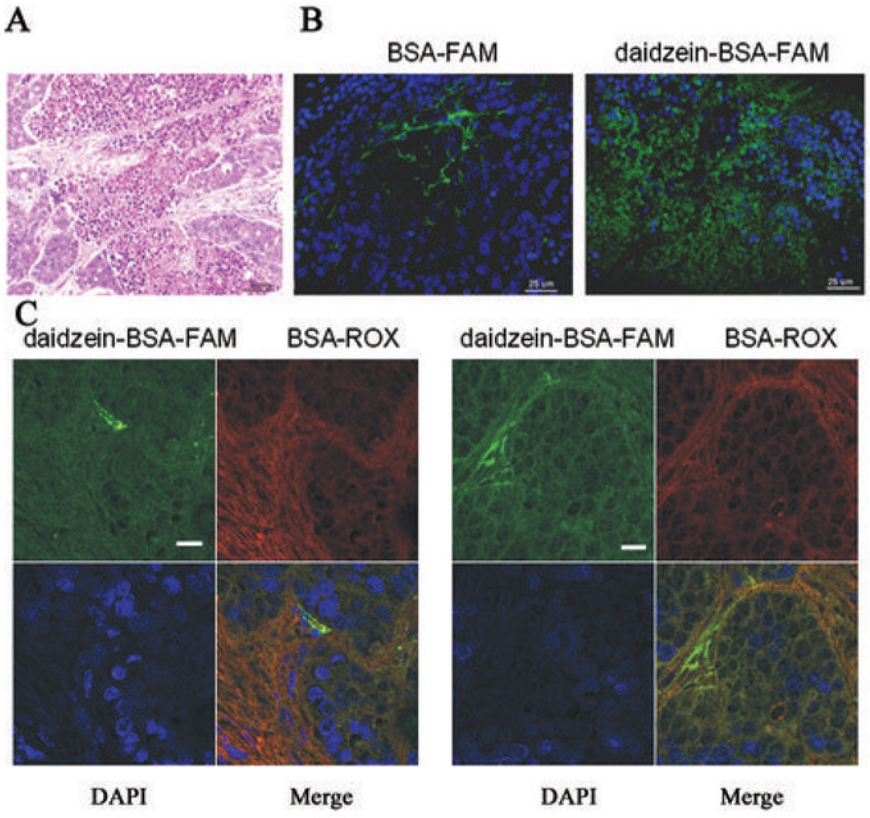

Figure 5. Ex-vivo characterization of contrast material distribution inside the tumor

MLS bearing mice were injected with BSA-FAM or Daidzein-BSA-FAM or combination of Daidzein-BSA-FAM and BSA-ROX. Tumors were isolated 24h after injection, fixed in Carnoy and imbedded in paraffin blocks. A) H&E staining of the tumor. Histological sections were stained with DAPI and visualized by fluorescence microscopy. B) Section of a tumor from a mouse injected with BSA-FAM or with Daidzein-BSA-FAM (green, FAM; blue, DAPI). C) Tumor sections derived from a mouse injected with daidzein-BSA-FAM and BSA-ROX (green, FAM; red, ROX; blue, DAPI).

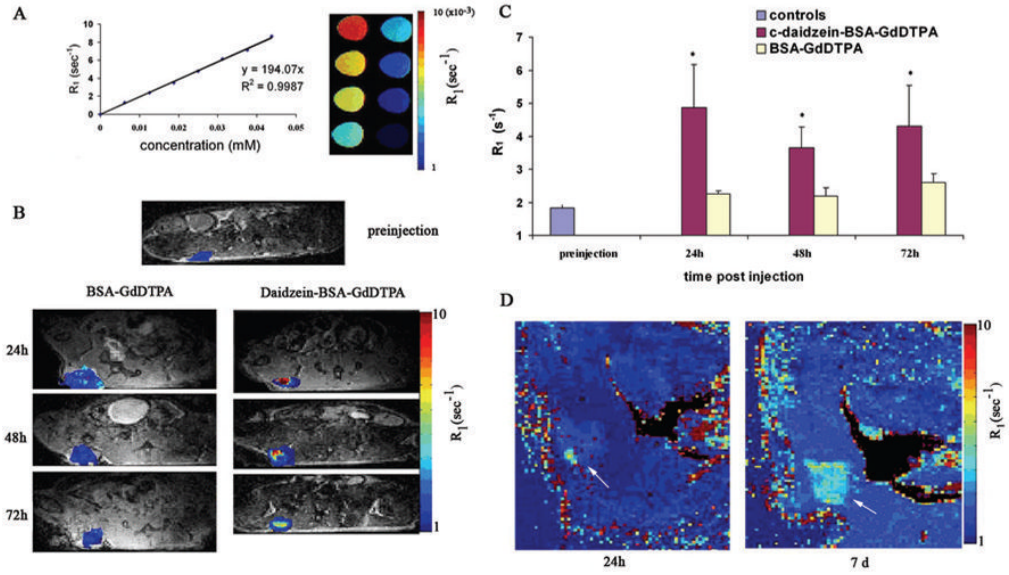

Figure 6. Daidzein-BSA-GdDTPA as a contrast material to MRI

A) The specific R_1 relaxivity of daidzein-BSA-GdDTPA was measured to be 194 $mM^{-1}s^{-1}$ per BSA. B), C) Specific localization and retention of the contrast material inside the tumor: MLS bearing mice were administered intravenously with 12mg BSA-GdDTPA (left) or daidzein-BSA-GdDTPA (right). T1 weighted MRI images and R_1 maps were obtained 24, 48 and 72h after injection, and used for derivation of mean R_1 values for the tumor. ROI analysis of MLS tumors of mice injected with BSA-GdDTPA (left) or daidzein-BSA-GdDTPA (right) and control (preinjection). * Significant differences in comparison of treatments (Student ttest $p<0.05$). D) Specific localization and retention of the contrast material inside the tumor: MLS tumor bearing mice were administered intravenously with 4.5mg daidzein-BSA-GdDTPA. R_1 maps were obtained 24h and 7d after injection.